

1 **Characterizing and modeling seasonality in extreme rainfall**

2 ^{1*}Theano Iliopoulou, ¹Demetris Koutsoyiannis and ²Alberto Montanari

3 ¹Department of Water Resources, Faculty of Civil Engineering, National Technical University of
4 Athens, Heroon Polytechniou 5, GR-157 80 Zografou, Greece

5 ²Department of Civil, Chemical, Environmental and Materials Engineering, University of
6 Bologna, Bologna, Italy

7
8 * Corresponding author. Tel.: +30 6978580613

9 *E-mail address:* anyi@central.ntua.gr

10

11 **Key points**

- 12 • The impact of seasonality on the tail index of the probability distribution of extreme
13 rainfall is minimal.
- 14 • Estimation uncertainty of extreme rainfall is relevant even when long historical records are
15 available.
- 16 • Estimating seasonality in extreme rainfall by dividing the year in 4 seasons leads to
17 overfitting and increased uncertainty.

18

19 **Plain language summary**

20 Climate studies and hydrological applications, e.g. flood risk mitigation, scheduling of season-
21 specific engineering works and reservoir management, often require information on the time of
22 occurrence and magnitude of extreme rainfall throughout the year. The seasonal variation of
23 rainfall extremes is investigated in a dataset of 27 remarkably long records including at least 150
24 years of daily measurements. An innovative method is proposed to perform identification of
25 seasons and simulation of extreme rainfall values for each season. Identification of the number of

26 seasons is achieved by evaluating alternative seasonal models according to model selection
27 criteria. Seasonal partitioning is performed by grouping consecutive months with similarly
28 behaving rainfall extremes. To generate synthetic data, extreme value probability distributions
29 are employed. The results indicate that seasonal properties of rainfall extremes mainly affect the
30 average values of seasonal maxima, while the shape of their probability distribution and its tail
31 do not substantially vary from season to season. Uncertainty in the estimated probability
32 distributions is important when comparing results from three different estimation methods, even
33 for long records, where one would expect that uncertainty is limited. The overall effectiveness of
34 the methodology is highlighted when contrasted to the conventional approach of using fixed
35 climatological seasons.

36

37 **Abstract**

38 A comprehensive understanding of seasonality in extreme rainfall is essential for climate studies,
39 flood prediction and various hydrological applications such as scheduling season-specific
40 engineering works, intra-annual management of reservoirs, seasonal flood risk mitigation and
41 stormwater management. To identify seasonality in extreme rainfall and quantify its impact in a
42 theoretically consistent yet practically appealing manner, we investigate a dataset of 27 daily
43 rainfall records spanning at least 150 years. We aim to objectively identify periods within the
44 year with distinct seasonal properties of extreme rainfall by employing the Akaike Information
45 Criterion (AIC). Optimal partitioning of seasons is identified by minimizing the within-season
46 variability of extremes. The statistics of annual and seasonal extremes are evaluated by fitting a
47 generalized extreme value (GEV) distribution to the annual and seasonal block maxima series.
48 The results indicate that seasonal properties of rainfall extremes mainly affect the average values
49 of seasonal maxima and their variability, while the shape of their probability distribution and its

50 tail do not substantially vary from season to season. Uncertainty in the estimation of the GEV
51 parameters is quantified by employing three different estimation methods (Maximum
52 Likelihood, Method of Moments and Least Squares) and the opportunity for joint parameter
53 estimation of seasonal and annual probability distributions of extremes is discussed. The
54 effectiveness of the proposed scheme for seasonal characterization and modeling is highlighted
55 when contrasted to results obtained from the conventional approach of using fixed climatological
56 seasons.

57 **Keywords:** seasonality, extreme daily rainfall, AIC, seasonal clustering, Generalized Extreme
58 Value Distribution, long rainfall records

59 **1. Introduction**

60 Seasonality is a dominant feature of most hydrological processes including extreme rainfall
61 (Hirschboeck, 1988). It implies intra-annual periodic variability which pertains to both timing
62 and magnitude of extreme rainfall. An accurate and effective characterization of seasonality is
63 critical to a wide variety of hydrological applications. For instance, it is useful in the scheduling
64 of various flood preparedness measures, including management of stormwater infrastructures
65 (Dhakal et al., 2015) and reservoir operation (Chiew et al., 2003; Fang et al., 2007; Chen et al.,
66 2010a). Similarly, seasonality characterization is exploited in advanced schemes of flood-
67 frequency analysis incorporating causative mechanisms (e.g. Sivapalan et al., 2005; Li et al.,
68 2016) and may be useful for medium-range flood prediction (e.g. Koutsoyiannis et al., 2008;
69 Wang et al., 2009; Aguilar et al., 2017), for which inclusion of seasonal extreme rainfall may
70 increase prediction skill. Modeling of seasonal rainfall extremes – which typically implies some
71 sort of frequency analysis – may also inform the selection of design values for related
72 infrastructure. Additionally, the latter provides support to within-year operation of water
73 resources systems, design rainfall estimation (Golian et al., 2010; Efstratiadis et al., 2014) and
74 probabilistic assessment of extreme events occurring in a given season. Nowadays, extreme
75 rainfall seasonality also prompts renewed scientific interest as a field of trend analyses (Ntegeka
76 and Willems, 2008; Dhakal et al., 2015; Tye et al., 2016; Wu and Qian, 2017).

77 Characterization of extreme rainfall seasonality is scarcely dealt with by the relevant
78 literature. Most of the established methods are devised to identify the temporal span of a wet
79 season and assess its significance, typically by a priori identifying a single wet season. For
80 example, directional statistics are typically applied to identify the high flow season (Cunderlik et
81 al., 2004a; Baratti et al., 2012; Chen et al., 2013) and have also been applied to characterize the

82 timing of seasonal rainfall (Parajka et al., 2009, 2010; Lee et al., 2012). However, directional
83 statistics are inefficient when extremes occur over multiple seasons, which is very likely in the
84 case of rainfall (Cunderlik and Burn, 2002). Recently, Dhakal et al. (2015) provided an
85 improvement to the traditional method of directional statistics by adopting a non-parametric
86 approach to capture multiple modes in the timing of annual rainfall maxima. Yet they noted that
87 the proposed method is sensitive to the subjective selection of threshold values to assess
88 significance of circular density estimates. Multimodality of the seasonal regime is also dealt with
89 by analyzing the monthly relative frequencies of extreme occurrences (Cunderlik and Burn,
90 2002; Cunderlik et al., 2004b). This approach, however, relies on the subjective identification of
91 the monthly time step to characterize seasonality. The latter along with the four climatological
92 seasons are often used when large-scale or global analyses are performed (e.g. Rust et al., 2009;
93 Villarini, 2012; Serinaldi and Kilsby, 2014; Papalexiou and Koutsoyiannis, 2016) but lead to
94 disregarding the large spatial variability of atmospheric patterns and may not align well with
95 local behaviors (Pryor and Schoof, 2008; Dhakal et al., 2015). Moreover, the fixed partitions do
96 not resolve the crucial question of the identification of the optimal number of seasons, therefore
97 resulting in over-parameterization of the seasonal model of extremes due to the large number of
98 seasons that is adopted, particularly in the 12 month model.

99 A sub-optimal characterization of seasonality could be a reasonable compromise when one
100 is interested in characterizing the timing of the most extreme events only. However, technical
101 applications often require the modeling of the frequency of extremes during the whole course of
102 the year. In this regard, several previous studies have either considered climatological
103 information or employed statistical methods along with some degree of subjective judgement to
104 estimate the optimal number of seasons and their displacement in time (e.g. Durrans et al., 2003;

105 Chen et al., 2010a; Baratti et al., 2012; Bowers et al., 2012). Coles et al. (2003) adopted a
106 different approach by treating seasonal temporal limits as unknown parameters to be identified
107 within a Bayesian framework. Yet, they also identified the number of seasons a priori through
108 subjective inference.

109 The above literature review highlights a methodological gap in the objective identification
110 of the optimal number of extreme rainfall seasons and their duration. To the best of the authors'
111 knowledge, existing methods are not suitable for directly inferring multimodality from the
112 seasonal regime and concurrently identifying segmentation points between seasons in an
113 objective manner.

114 The research herein presented proposes a two-purpose framework for (a) objective
115 seasonality identification and (b) modelling of rainfall extremes in order to effectively estimate
116 the seasonal probability of extreme events. To this end, we introduce two alternative methods for
117 season identification, which are characterized by different levels of parsimony in terms of data
118 requirements, therefore providing two options for practical applications. Our approach employs
119 an information-theoretic framework (Akaike Information Criterion, AIC) to estimate the optimal
120 number of seasons. In order to describe the frequency of extremes in each identified season we
121 use the GEV probability distribution. We discuss the consistency of the model at different time
122 scales. Finally, in order to demonstrate the efficiency of our framework we present a comparison
123 with the traditional 4-season approach.

124 An extended dataset of long daily rainfall records is herein investigated, as detailed in the
125 next section. The length of the records, the shortest one covering an observation period of 150
126 years, allows us to inspect the impact of uncertainty, which may be relevant for seasonal extreme
127 value analyses (Cunderlik et al., 2004c). To reduce uncertainty we propose a robust

128 parameterization approach of seasonal-annual distributions which is supported by empirical
129 evidence.

130 **2. Dataset**

131 Our dataset includes 27 daily rainfall records each one spanning over 150 years. Eighteen of
132 them are collected from global databases, namely, the Global Historical Climatology Network
133 Daily database (Menne et al., 2012) and the European Climate Assessment & Dataset (Klein
134 Tank et al., 2002). Figure 1 shows the geographical location of the stations, while Table 1 reports
135 the coordinates of each station, the observation period, as well as the number of years that are
136 fully covered by observations after quality control and screening of missing values. For the
137 extraction of the annual maxima we employ a methodology proposed by Papalexiou and
138 Koutsoyiannis (2013); accordingly, an annual maximum is not accepted if (a) it belongs to the
139 lowest 40% of the annual maxima values and (b) 30% or more of the observations for that year
140 are missing. For seasonal and monthly maxima we compute statistics only if number of missing
141 values is less than 10% of the total sample (season or month). The longest series is that of Padua,
142 that is, the longest rainfall record existing worldwide (Marani and Zanetti, 2015).

143 **3. Methodology**

144 **3.1 Season identification**

145 The methodology that we propose to identify seasons is inspired by cluster analysis and model
146 selection techniques. Seasons are regarded as groups (clusters) of consecutive months with
147 similar behavior of extremes. The question of selecting the number of seasons that best describe
148 the dataset is addressed here via a model selection process under the assumption that different
149 numbers of clusters (seasons) represent alternative plausible models for the dataset. Two

150 alternative methods for season identification characterized by different level of parsimony are
 151 considered here and described below.

152 In what follows, we denote random variables and their realizations by upper and lower case
 153 symbols, respectively. We also use bold characters for vectors. We denote season, month and
 154 year with the indexes $i = 1, \dots, n$, $j = 1, \dots, 12$, and $k = 1, \dots, k_{\max}$, respectively, where n is the number of
 155 seasons and k_{\max} is the record length in years. We assume that n is fixed a priori and denote with
 156 c_i the vector containing the j values of contiguous months belonging to the same season i , and
 157 with s_i its size. Accordingly, we define the following random variables:

- 158 • $R_{i,j,k}$ is the maximum daily rainfall amount of season i , month j and year k ;
- 159 • $R_{i,j}$ is the temporal average of maximum daily rainfall of month j of season i along the
 160 record, namely, $R_{i,j} := \frac{1}{k_{\max}} \sum_{k=1}^{k_{\max}} R_{i,j,k}$;
- 161 • R_i is the temporal average of the $R_{i,j}$ values along the season i , $R_i := \frac{1}{s_i} \sum_{j \in c_i} R_{i,j}$.

162 For instance, $r_{2,5,12}$ for season $i=2$ defined by $c_2 = [5,6,7]$ denotes the maximum daily
 163 rainfall observed in May of the 12th year of a given record and belonging to the 2nd identified
 164 season of the year, which also includes months June and July; likewise, $r_{2,5}$ is the sample average
 165 of maximum rainfall observed in all May days of the record, while, r_2 is the sample average of all
 166 monthly averages belonging to season 2, in this case of May, June and July.

167 We call the first method for season identification the SSD algorithm. It is based on the
 168 computation of Sum of Squared Deviations (SSD) of the $R_{i,j}$ values from their seasonal average,
 169 R_i for all seasons according to the equation:

$$170 \quad \text{SSD} = \sum_{i=1}^n \sum_{j \in c_i} (R_{i,j} - R_i)^2 \quad (1)$$

171 This metric is evaluated for each possible clustering combination c_i of consecutive months for
172 the given number of seasons, thus enabling the identification of the lower value of SSD, which
173 identifies the optimal partition of the year into n seasons. We require a season to span at least
174 two months and allow the algorithm to group months across different calendar years. The
175 requirement for a season to span at least two months implies that the maximum number of
176 seasons is 6, but preliminary investigations showed that more than three seasons are rarely
177 present in extreme rainfall. Therefore, we limit our attention to n values ranging in the interval
178 [1-4].

179 Essentially, the SSD algorithm minimizes the within-cluster variance of the average value
180 over the years of the monthly rainfall maxima and can be considered as a simplification of the
181 well-known k -means algorithm (MacQueen, 1967). Since seasons may include contiguous
182 months only, and the algorithm deals with only 12 data points to cluster - the average over the
183 years of daily maximum rainfall values for each month - the number of possible combinations is
184 relatively low and the method is parsimonious.

185 In order to identify the optimal number of seasons we define alternative probabilistic
186 models, with different level of parsimony, to describe the frequency of occurrence of extreme
187 events in each season and assess their ability to optimally fit the observed record. Accordingly,
188 we first select a trial value for the number n of seasons in the range [1-4] and partition them by
189 applying the above SSD algorithm. To describe the probability distribution of rainfall in each
190 season and the whole year we form a mixture model with n seasonal components, each described
191 by its own probability distribution. Hence, according to the law of total probability, the
192 probability distribution of the seasonal model for a generic seasonal random variable U takes the
193 form:

194
$$f_U(u; \mathbf{a}_1, \dots, \mathbf{a}_n) = \sum_{i=1}^n w_i f_{U_i}(u_i; \mathbf{a}_i) \quad (2)$$

195 where w_i are weights adding up to 1. They are obtained as the ratio of the season's length in
 196 months, s_i , versus the whole twelve-month period, i.e. $w_i = s_i/12$; and \mathbf{a}_i is a seasonal parameter
 197 vector. Here f_{U_i} is a seasonal probability distribution for U describing realizations u_i in season i .
 198 Note that by applying the law of total probability instead of deriving the annual probability
 199 distribution as the product of the seasonal ones, we avoid relying on the assumption of
 200 independence of the random variables U_i , which was adopted in other studies (Durrans et al.,
 201 2003). Therefore, this is a more general approach also appropriate for the rarer cases of rainfall
 202 maxima being correlated among seasons.

203 The above step requires identifying and fitting a candidate model for the f_{U_i} probability
 204 distribution. We propose two alternative models for the seasonal probability distribution $f_{U_i}(u_i,$
 205 $\mathbf{a}_i)$ which are characterized by different level of complexity.

206 The first option, which we call Average Based (AB) method, identifies the random variable
 207 U_i as the monthly temporal average $R_{i,j}$. Then, we assume that $f_{R_{i,j}}(r_{i,j}, \mathbf{a}_i)$ is a uniform
 208 distribution given by:

209
$$f_{R_{i,j}}(r_{i,j}, \mathbf{a}_i) = \frac{1}{b_i} \quad (3)$$

210 where in this case \mathbf{a}_i contains only one parameter, namely, $b_i = \max_{j \in \mathcal{C}_i} r_{i,j}$. Preliminary analyses
 211 showed that the uniform distribution provides an efficient representation of the frequency of the
 212 $r_{i,j}$ realizations, by minimizing the number of involved parameters. The above approach imposes
 213 an upper limit to the average value of the monthly maximum rainfall depth and sets the lower
 214 limit to zero.

215 The second option, which we call Complete Data (CD) method, identifies the random
 216 variable U_i as the maximum daily rainfall in each month j of the season i for the year k , which
 217 has been previously introduced as $R_{i,j,k}$. Then, we assume that $f_{R_{i,j,k}}(r_{i,j,k}, \mathbf{a}_i)$ is described by two
 218 alternative probability distributions with a different tail behavior, i.e. one characterized by a
 219 lighter and one by a heavier right tail, in order to allow flexibility in fitting the observed rainfall
 220 maxima. The first is the two-parameter Gamma distribution, given by:

$$221 \quad f_{R_{i,j,k}}(r_{i,j,k}, \mathbf{a}_i) = \frac{r_{i,j,k}^{\xi_i-1} e^{-\frac{r_{i,j,k}}{\theta_i}}}{\theta_i^{\xi_i} \Gamma(\xi_i)} \quad (4)$$

222 where $\mathbf{a}_i = (\zeta_i, \theta_i)$ is the parameter vector with ζ and θ being shape and scale parameters,
 223 respectively. The second is the two-parameter Weibull distribution:

$$224 \quad f_{R_{i,j,k}}(r_{i,j,k}, \mathbf{a}_i) = \frac{\mu_i}{\lambda_i} \left(\frac{r_{i,j,k}}{\lambda_i} \right)^{\mu_i-1} e^{-(r_{i,j,k}/\lambda_i)^{\mu_i}} \quad (5)$$

225 where $\mathbf{a}_i = (\mu_i, \lambda_i)$ is the parameter vector with μ and λ being shape and scale parameters,
 226 respectively. By working on the monthly maximum rainfall instead of their averages along the
 227 season, the CD method allows one to base the estimation of the probability model on a more
 228 extended dataset.

229 The above methodology allows several modeling options, which differ for the number of
 230 seasons, the application of either AB or CD method and the selection of either the Gamma or the
 231 Weibull distribution in the CD method. The best modeling option and the related optimal number
 232 of seasons is identified by applying the Akaike Information Criterion (AIC, Akaike, 1973, 1974).
 233 The criterion statistic for the p th candidate model, AIC_p , is given by:

$$234 \quad AIC_p = 2m_p - 2\ln L_p \quad (6)$$

235 where m_p is the number of parameters and L_p is the likelihood of the p th candidate model. The
236 application of the criterion is straightforward as it only requires estimation of the likelihood
237 function for the candidate probability models defined by eq. (2). The minimum AIC value
238 identifies the best candidate model by evaluating the bias versus variance trade off; i.e., the
239 condition in which as the model parameters increase the bias of the model estimates decreases,
240 yet their variance increases (Burnham and Anderson, 2002). Hence, AIC provides an implicit
241 interpretation of the principle of parsimony which is pivotal in model selection (Box and Jenkins,
242 1970). Although AIC has a solid foundation in information theory both in mathematical terms
243 and also from a philosophical point of view, its use is not still widely established in hydrological
244 applications (Laio et al., 2009). For an insightful review of AIC's properties, the reader is
245 referred to Burnham and Anderson (2002).

246 Therefore, the workflow for season identification is as follows:

- 247 1. A trial value is adopted for the number n of seasons in the range [1-4];
- 248 2. The n seasons are partitioned by applying the SSD algorithm therefore identifying the
249 vectors $c_i, i = 1, \dots, n$, of the indexes of the months that are included in each season;
- 250 3. AB and CD methods are applied to estimate the probability distribution of $R_{i,j}$ and $R_{i,j,k}$,
251 respectively, in each season;
- 252 4. AIC is computed for candidate models;
- 253 5. The procedure is repeated for the other values of n in the range [1-4];
- 254 6. The resulting AIC values are compared therefore identifying the optimal number of
255 seasons, and their partition, for AB and CD methods.
- 256 7. If n values resulting from AB and CD methods are the same, then the procedure is
257 terminated and the optimal partition of seasons is uniquely identified;

258 8. If the estimated n values differ, then the user is allowed to select the preferred partition of
259 seasons based on the suitability of $R_{i,j}$ instead of $R_{i,j,k}$, for the considered design problem.

260 3.2 Extreme value analysis

261 3.2.1 Fitting the GEV distribution

262 Once the optimal number of seasons and their partition have been identified, to estimate seasonal
263 extremes one needs to fit a suitable probabilistic model for the seasonal block maxima series.
264 The latter is formed by extracting from each identified season the maximum daily rainfall
265 observed in each year. It is worth noting that distributions that were previously considered for
266 seasonal partitioning (the Gamma and the Weibull) are not suited for fitting extreme values and
267 therefore are not an option for the current target.

268 Extreme Value Theory (EVT) suggests that the distribution of the maximum of ν
269 independent and identically distributed (i.i.d.) random variables asymptotically converges to
270 three limiting laws (Fisher and Tippett, 1928), which are the Gumbel distribution (Type I), the
271 Fréchet distribution (Type II) and the reversed Weibull (Type III), that can be unified under the
272 following single analytical form provided independently by von Mises (1936) and Jenkinson
273 (1955) and known as Generalized Extreme Value (GEV) distribution:

$$274 \quad G_X(x) = \exp\left(-\left(1 + \kappa \frac{x - \psi}{\sigma}\right)^{\frac{1}{\kappa}}\right), \quad 1 + \kappa \frac{x - \psi}{\sigma} \geq 0 \quad (7)$$

275 where X is a generic random variable and $\kappa \in \mathbb{R}$ is a shape parameter, $\sigma > 0$ is a scale parameter
276 and $\psi \in \mathbb{R}$ is a location parameter. The Type I distribution emerges for $\kappa = 0$, the Type II for $\kappa >$
277 0 , while the Type III emerges as the limiting distribution for $\kappa < 0$, but it is not used for modeling
278 rainfall extremes as it is upper limited. GEV is the limiting distribution for extremes from any
279 parent distribution of the underlying stochastic process. Therefore, it could be the limiting

280 distribution also in the case of monthly rainfall maxima described by the Gamma and Weibull
281 distributions as in the CD method above. Leadbetter (1974) showed that convergence to GEV is
282 guaranteed even in the presence of short-range correlation in the underlying stochastic process.
283 In our case, the implication is that GEV emerges as limiting distribution even if rainfall maxima
284 are correlated. Koutsoyiannis (2004a) has shown mathematically that GEV still emerges as
285 asymptotical distribution in the presence of different parent distributions from season to season.
286 In practical applications, though, in which a maximum value is extracted from a small number of
287 events, the asymptotic condition is unlikely to hold. In this respect, Koutsoyiannis (2004a)
288 demonstrated that the convergence of the distribution of maxima to the GEV with a positive
289 shape parameter (Type II) is good even for a small number of events and also for parent
290 distributions belonging to the domain of attraction of the Gumbel (Type I), due to the increased
291 flexibility of the three-parameter distribution. On the contrary, convergence rates to the Gumbel
292 distribution are very slow even for distributions belonging to the domain of attraction of the
293 Gumbel family (see also Papalexiou and Koutsoyiannis, 2013).

294 Here, we assume that the underlying stochastic process is given by the series of the
295 monthly maxima of daily rainfall in each season. We aim to fit with the GEV distribution the
296 seasonal samples that are obtained by extracting from each season i and each year k the
297 maximum daily value $r_{i,k}^*$ therefore obtaining a block maxima series, which is assumed to be a
298 realization of the random variable $R_{i,k}^*$. We also fit the series of the annual maxima r_k^* which is
299 assumed to be a realization of the random variable R_k^* . This approach shall allow one to estimate
300 the extremes for the seasonal periods and the total annual period and ensures that both the
301 seasonal and annual approaches refer to the same sample size when fitting the GEV, as the block

302 maxima sampling method is used, i.e., one extreme event is sampled on a yearly basis for both
303 the seasonal and annual periods.

304 *3.2.2. Investigating consistency of seasonal and annual distributions*

305 A considerable part of related literature (e.g. Buishand and Demaré, 1990; Durrans et al., 2003;
306 Chen et al., 2010b; Baratti et al., 2012) has focused on the estimation of seasonal and annual
307 flood frequency distributions and their inter-relationship. Usually, it is suggested that an
308 independent fitting of seasonal and annual distributions may lead to inconsistency among them,
309 manifested as a “crossing over” effect. The latter means that for extremely rare events seasonal
310 quantiles may be higher than their annual counterparts. To resolve this inconsistency, a variety of
311 methods for the joint estimation of the seasonal and annual distributions has been proposed.

312 Durrans et al. (2003) attributed distributional inconsistencies in seasonal-annual frequency
313 analysis to three possible reasons: (a) the arbitrary parameterization of seasonal and annual
314 distributions, (b) stochastic dependence among them and (c) estimation uncertainty. In this
315 respect, we believe that the arbitrary specification of seasonal samples is also a major reason
316 causing distributional inconsistencies (such a case is discussed and illustrated later in section
317 4.5). In our case though, we argue that the above inconsistency should rather be viewed as an
318 empirical evidence of estimation uncertainty, which is particularly relevant in extreme value
319 studies (Coles et al., 2003; Koutsoyiannis, 2004a). This is further supported by observing that the
320 crossing over effect is manifested in the domain of extremely rare events, where uncertainty is
321 prominent.

322 To inspect the impact of estimation uncertainty, we fit the GEV probability distribution by
323 applying three different methods, namely, maximum likelihood (ML), method of moments (MM)
324 and a least squares estimation method (LS) for an improved fitting of the extremes

325 (Koutsoyiannis, 2004b). We further investigate estimation uncertainty in each of the three
326 methods by computing 95% Monte Carlo Prediction Limits (MCPL) for the resulting GEV
327 quantiles. MCPL are estimated by applying a Monte Carlo simulation which is structured
328 according to the following steps: (1) we estimate the GEV parameters by each method, (2)
329 produce 1000 synthetic GEV series for each derived parameter set, (3) re-estimate the parameters
330 by the same method, (4) compute the resulting GEV quantiles for each of them and then (5)
331 identify the 95% confidence region for each quantile value. The scope is to assess whether the
332 crossing over falls within the limits of the estimation uncertainty as evaluated from applying a
333 set of different parameter estimation methods. To further reduce fitting uncertainty, we propose a
334 simpler alternative to joint parameterization, i.e. the joint estimation of a common shape
335 parameter among seasonal-annual distributions – since the shape parameter is the most difficult
336 to estimate accurately – and we discuss how this choice is supported by empirical evidence.

337

338 **4. Results**

339 **4.1 Season identification for the observed records**

340 Table 2 shows the AIC values resulting from season identification for the available stations.
341 Following Burnham and Anderson (2004), we denote with ΔAIC the difference in the AIC value
342 of each model with respect to the best one. Therefore, the zero ΔAIC model is the best model,
343 while models with $\Delta AIC < 2$ and $\Delta AIC > 10$ are assumed to have good and little support,
344 respectively. An example of seasonal partition for the case of Florence is shown in Figure 2a and
345 Figure 2b for 2 and 3 seasons. We refer to this type of figures as *climatograms*, though the term
346 is typically used for plots depicting both rainfall and temperature climatological regimes.

347 The results point out that both methods identified the one-season (annual) model as the
348 best solution for 11 stations (with 6 stations being the same for both methods). In four stations,
349 the one-season model was preferred by the CD method, while the two-season solution was
350 indicated by the AB method. On further investigation, it was found that neither the Gamma, nor
351 the Weibull provided satisfactory likelihood values for these stations. As a result, the more
352 parsimonious one-season model was preferred by the AIC. The three-season model is identified
353 as the best solution for five stations with the CD method, while the AB method did not select
354 $n = 3$ for any station. This result was expected as the AB method exploits information from a
355 limited dataset and therefore parsimonious models are likely to provide better AIC values. The
356 Gamma distribution is selected as the best model in 21 cases and the Weibull for the remaining
357 6.

358 To inspect the spatial coherence of the results, we present maps of the two regions of the
359 dataset having neighboring stations, i.e. Europe and Australia (Figure 3). We group the stations
360 in six clusters of similarity in their seasonal patterns and we also mark single stations for which
361 similarity falls below the accepted threshold. As similarity index we define the ratio of the
362 number of the wet season months that the stations in the cluster have in common versus the span
363 of each wet season and we require it to be at least 60% for each station in the cluster. More
364 specifically, Clusters 1 and 2 have 67% and 80% similarity, respectively, for both methods,
365 while, Clusters 3, 4 and 5 exhibit 100%-75%, 60%-75% and 80%-67% for the AB and CD
366 methods, respectively. On top of the maps, we also plot Köppen maps of climate classification
367 by Chen and Chen (2013) covering the period 1901-2010, in order to allow a direct comparison
368 of the observed spatial patterns to the climatological ones. Some interesting insights can be
369 derived. First, spatial coherence does not fully coincide with climatological coherence and vice

370 versa, and this is especially true in regions with complex topography/climatology. For example,
371 in the wider Alpine region, where climate shows great diversity, the stations are less spatially
372 consistent than in Central Europe. On the contrary, stations belonging to a Mediterranean climate
373 (Cluster 1) show consistent patterns. In general, we notice that patterns are coherent on both
374 levels: neighboring stations show very high similarity (e.g. Cluster 3) and far apart stations
375 belonging to a climatically homogenous region show medium to high similarity (see, e.g.,
376 Cluster 2).

377

378 **4.2 Assessing temporal change in observed seasonality**

379 To demonstrate the applicability of the proposed season identification method in the inspection
380 of temporal changes in seasonality, we analyze the four longest records of the dataset, i.e. the
381 stations of Padua (275 years), Prague (211 years), Bologna (195 years) and Radcliffe (188
382 years). We split the observation period into equally sized sub-periods and apply the methodology
383 independently to each period. We employ four sub-periods for the significantly longer station of
384 Padua and three for the other records.

385 Results are shown in Table 3. It can be seen that changes, both in the number and duration
386 of seasons, are likely to emerge within each sub-period. For example, seasonality in Prague
387 during the 2nd period changed in terms of the span of the wet season, but a two-season regime
388 was selected for all sub-periods. Results for 3rd and 1st window coincide. These characteristics of
389 the methodology make it useful for climate change analysis.

390

391 **4.3 Fitting the GEV distribution**

392 Subsequently to the identification of seasons, we fitted the GEV distribution via maximum
393 likelihood (ML) estimation to each of the seasonal sets (or the annual set if one season was
394 identified). Table 4 contains summary statistics of the GEV fitting for wet and dry seasons, as
395 well as for the whole year, for the cases where the two- and three-season model were found
396 prevalent under AB and/or CD methods. Summary statistics for the transition season (placed
397 between the wet and dry season) in the three season model are omitted since the sample is small
398 (5 stations). The main differences in the seasonal distributions lie in the values of the scale and
399 location parameters, which are in their vast majority (93.8% and 100%, respectively, under AB
400 method and 100% and 100%, respectively, under CD method) higher for the wet season
401 compared to the dry. What might be less anticipated is that there is limited seasonal variation in
402 the value of the shape parameter κ , which is related to the shape of the tail of the seasonal
403 maxima distribution. Hence, it is justifiable to represent the two seasons and the whole year by a
404 common value for the shape parameter, therefore increasing robustness of the method, which is a
405 desirable feature. Additionally, for the majority of the stations, the shape parameter takes
406 positive values indicating the appropriateness of heavier-tailed distributions for modeling of
407 extremes. It is also clear that the wet extreme properties are quite close to the annual maxima
408 ones, which indicates that the annual maxima distribution is dominated by the wet season.

409 The singular cases of the stations of Prague from Czech Republic and Florence from Italy
410 are plotted in Figures 4a and 4b. In the second case, there is small deviation between the wet
411 season and the annual period, while in the first case the two lines are almost identical. In both
412 cases, the dry-season probability line lies considerably lower. In the second case, in which the
413 three-season model is preferred by the CD method (while two seasons were preferred by the AB

414 method), the probability line of the transition season lies in the space between the wet and dry
415 seasons' probability lines, as expected.

416

417 **4.4 Assessing estimation uncertainty in seasonal-annual GEV parameterization**

418 The crossing over effect mentioned in Section 3.2.2 is observed in five cases (Eelde, Genoa,
419 Hohenpeissenberg, Milan and Zagreb), where we found that the wet-season probability
420 distribution lies higher than the annual one in the area of extremely rare events. We focus on the
421 station in Genoa where the effect is more pronounced. As mentioned in Section 3.3, we
422 performed additional parameter estimation by applying the method of moments (MM) and the
423 least squares algorithm (LS). Figure 5a shows results from the application of the three estimation
424 methods for the annual maximum series along with uncertainty bounds computed within each
425 method by means of Monte Carlo analysis. Uncertainty bounds in the area of extremely rare
426 events, where the crossing over effect is also observed, are large. The larger annual maxima fall
427 within the 95% limits of the annual maxima GEV distribution only for the LS method. This is
428 due to the better fitting capability of the LS algorithm for extremely rare events (Koutsoyiannis,
429 2004b). To further improve the fitting we also estimate via LS a common shape parameter for
430 the three distributions (two seasonal GEV and the annual one). In these cases as well, the choice
431 of a common shape parameter is supported by empirical evidence from the previous independent
432 fitting. The crossing over effect is significantly mitigated (Figure 5b), with a remaining positive
433 difference between the quantiles of the wet season and annual distribution of 10 mm for the 0.5%
434 annual exceedance probability, which is considered not significant in view of the large
435 uncertainty in the high-quantile domain. The results for the other cases also showed that the
436 crossing over effect was resolved.

437 The importance of taking estimation uncertainty into consideration is additionally
438 showcased by applying ML, MM and LS estimation methods to the entire set of stations, as
439 shown in Table 5. One notices that uncertainty is higher in the estimation of the shape parameter,
440 as already discussed in literature (Koutsoyiannis, 2004b; Papalexiou and Koutsoyiannis, 2013).
441 The fact that this result is empirically confirmed for the long rainfall records considered here is a
442 further confirmation that for practical applications uncertainty in the estimation of extremes is
443 unavoidable even when dealing with long records.

444 **4.5 A comparison to traditional methods of seasonal clustering**

445 We compare our method to the climatological 4-season approach, which divides the annual
446 period in Winter, Spring, Summer and Fall seasons. First, to highlight that site-specific season
447 identification is important, we compare the monthly maxima plots for two stations in Europe for
448 our method and the fixed seasonal partition (Figure 6). It is clear that climatological seasons are
449 an inefficient partition for analyzing the extreme rainfall properties, and may also be a rather
450 crude method for delineating the extreme's properties in multi-site analyses where seasonal
451 differences in climate may be very pronounced among stations. As an example, seasonality of
452 maximum rainfall in Jena (Germany) is completely out of phase with respect to Athens (Greece).
453 The same could be argued for trend studies employing fixed characterizations of seasonality. For
454 instance, the question of whether winter rainfall has increased is potentially ill-conceived, as it
455 mostly pertains to a subjective interpretation of seasonality. A more relevant question is whether
456 rainfall in the major rainy season has significantly changed, but such a change is unlikely to be
457 identified by considering an arbitrary partition in seasons.

458 To demonstrate the effect that a fixed 4-season partition could have on the estimation of
459 extreme value properties, we focus on the rainfall record of Athens. By applying the 4-season

460 partition one obtains an apparent overfitting, as the seasonal lines are not clearly separated and
461 even cross each other at several points (Figure 7b). It is evident that an inappropriate
462 characterization of seasonality provides no valuable and practical information for seasonal
463 planning and decision-making while, in fact, it obscures the presence of the existing seasonal
464 regime (Figure 7a). Additionally, in the presence of parameter uncertainty and given the short
465 record lengths that are usually available, adopting subjective characterizations of seasonality for
466 the study of extreme values entails the risk of disproportionately increasing estimation
467 uncertainty. The consequences of overfitting are even more obvious in stations with very low or
468 no seasonality.

469

470 **5. Discussion and Conclusions**

471 An objective methodology is proposed to allow season identification in extreme daily rainfall
472 and the study of the resulting extreme properties in each season. The methodology is evaluated
473 on an extended dataset comprising 27 rainfall stations covering a period of more than 150 years
474 of daily observations. In the following, we discuss methodological and modeling issues, the
475 results of the extreme value analysis and their comparison to the no-seasonality approach, as well
476 as relative strengths and potential limitations of our method.

477 The season identification methodology herein proposed is based on the SSD algorithm, a
478 simplified version of the k -means clustering algorithm, whose results are evaluated by exploiting
479 the model selection properties of the Akaike Information Criterion (AIC). The method is able to
480 identify the optimal modeling option for the seasonal extreme rainfall for a given dataset,
481 discerning among the existence of 1 (no dominant season) to 4 seasons in the extreme rainfall
482 properties and identifying their temporal span. Since AIC is a measure of relative performance of

483 models, this task should be performed after thorough consideration of the appropriateness of the
484 candidate seasonal distributions to be assessed. In that respect, our methodology provides
485 additional flexibility as multiple probabilistic models may be simultaneously assessed. Overall,
486 the methodology shows good spatial coherence, which makes it potentially appropriate for
487 regionalization studies, and its flexibility allows one to inspect temporal changes in a range of
488 ways, which is also a desirable feature concerning climatic variability and trend studies.

489 In terms of generated results, the adopted scheme proved to be successful for the long
490 rainfall records considered here, by both visual evaluation of the plots of the monthly maximum
491 rainfall values (climatograms) and assessment of the resulting extreme seasonal distributional
492 properties. For the cases where two or three seasons are identified, the differences in the
493 distributional properties are reflected mainly in the value of the scale and location parameters of
494 the GEV which are significantly higher for the wet season. The shape parameter shows limited
495 seasonal variability, which implies that the seasonal distributional properties do not differ
496 substantially in the shape of the distribution tail. Our results also confirm other studies regarding
497 the prevalence of heavy-tailed distributions for daily rainfall extremes (Koutsoyiannis, 2004b;
498 Villarini, 2012; Papalexiou and Koutsoyiannis, 2013; Serinaldi and Kilsby, 2014; Mascaro,
499 2018). Some of these studies have also argued that a positive shape parameter emerges for
500 extremes caused by multiple types of synoptic patterns, whereas a zero exponent (i.e. an
501 exponential tail) may occur for a single-type of events. Apart from pronounced intra-annual
502 variability, a positive shape parameter may be also portraying increased inter-annual variability
503 in the extremes which has been linked to the presence of large-scale circulation patterns, i.e. the
504 NAO, for certain stations of our dataset (Kutiél and Trigo, 2014; Marani and Zanetti, 2015). In
505 principle, we believe that our findings are in agreement with previous research and strengthen

506 the assumption that a heavier-tail behaviour better captures conditions of enhanced natural
507 variability and complex atmospheric forcing, as revealed by the inspection of our long and
508 spatially sparse dataset.

509 In comparison to the no-seasonality approach, in some cases the annual maxima series are
510 found to be dominated by extreme events occurring in the wet season. This result is pointed out
511 by the closeness in the estimated GEV parameter values between the annual and the wet season's
512 probability distribution of extreme events. It also indicates that annual frequency analyses may
513 suffice for studying the annual maxima (AM). Actually, studying the AM series is more in favor
514 of a conservative design approach, since the former takes into account the rare cases of extreme
515 events of significant magnitude happening in the dry season. Furthermore, since the majority of
516 AM in records with pronounced seasonality still stems from the wet season, strong seasonality is
517 not significantly violating the i.i.d. assumption in the GEV approach. A similar remark was also
518 made by Allamano et al. (2011). However, for intra-annual hydrological design and
519 management, it is crucial to take seasonal variability into account. The wet season maxima series
520 contain valuable information on the timing of occurrence of the most extreme events, although it
521 is likely that in some cases, their magnitude will be close to the AM estimated one. Yet when dry
522 periods are of interest, using the AM series instead, i.e. adopting a no-seasonality approach, is
523 likely to lead to costly overestimation of design values and floodwater waste.

524 A few key strengths of our methodology should be underlined. In general, estimation
525 uncertainty in extreme studies is a known issue especially for the estimation of the shape
526 parameter of the GEV distribution. Here, we show how an alternative choice of estimation
527 methods, improving the model performance in the domain of extreme events, may resolve
528 inconsistencies deriving from an independent seasonal and annual fitting. Given the latter, we

529 consider the need for the laborious joint estimation of seasonal-annual distributions to be
530 questionable and we propose a simpler procedure based on the estimation of a common shape
531 parameter for the seasonal-annual parameterization, which is shown to increase robustness of the
532 statistical model. On the whole, the entire methodology is compared to a conventional partition
533 in fixed seasons and its advantageous features are highlighted both in that it enables consistent
534 identification of seasonal regimes at single-site and multi-site levels, as opposed to arbitrary
535 partitions, and that it consequently allows a more informed and parsimonious fitting of the GEV
536 distribution to seasonal extremes.

537 A few limitations should be taken into account. We note that in case where the Average
538 Based (AB) and the Complete Data (CD) methods diverge, there is some remaining degree of
539 subjectivity in the choice for the most appropriate scheme. This constitutes a potential limitation
540 of our method as results may not be fully conclusive. Yet this may be resolved if an equifinality
541 framework is adopted and both options are considered. Additionally, it should be noted that the
542 performance of AIC largely depends on the quality of the considered candidate models.
543 Although the chosen distributions are representative of a variety of statistical behaviors, it is
544 possible that there may be exceptions for which they do not perform well. Increasing the set of
545 candidate distributions is another option to achieve a greater degree of confidence within a multi-
546 model approach.

547 Despite these limitations, we believe that our findings have direct applications both in the
548 theoretical conceptualization of seasonality in extreme rainfall and in engineering applications.
549 On a methodological level, they contribute to a wider establishment of model selection
550 techniques, in this case AIC, in hydrological studies and pave the way for the objective

551 identification of seasonality via automated schemes which are required for global-scale
552 hydrology.

553 **Acknowledgments**

554 We greatly thank the Radcliffe Meteorological Station (Burt and Howden, 2011), the Icelandic
555 Meteorological Office (Trausti Jónsson), the Czech Hydrometeorological Institute, the Finnish
556 Meteorological Institute, the National Observatory of Athens, the Department of Earth Sciences
557 of the Uppsala University and the Regional Hydrologic Service of the Tuscany Region
558 (servizio.idrologico@regione.toscana.it) for providing the required data for each region
559 respectively. We are also grateful to Professor Ricardo Machado Trigo (University of Lisbon) for
560 providing the Lisbon timeseries and to Professor Marco Marani (University of Padua) for
561 providing the Padua timeseries. All the above data were freely provided after contacting the
562 acknowledged sources. The Eelde and Den Helder timeseries are publicly available by the data
563 providers in the ECA&D project (<http://www.ecad.eu>), while the remaining 16 timeseries can be
564 freely accessed at the GHCN-Daily database ([https://data.noaa.gov/dataset/global-historical-](https://data.noaa.gov/dataset/global-historical-climatology-network-daily-ghcn-daily-version-3)
565 [climatology-network-daily-ghcn-daily-version-3](https://data.noaa.gov/dataset/global-historical-climatology-network-daily-ghcn-daily-version-3)). We greatly thank Professor Marco Marani and
566 Professor Attilio Castellarin (University of Bologna) for their helpful discussions during an early
567 stage of this research. We are also grateful to the anonymous reviewers and the Associate Editor
568 for providing very constructive remarks and suggestions.

569 **References**

- 570 Aguilar, C., Montanari, A., Polo, M.-J., 2017. Real-time updating of the flood frequency
571 distribution through data assimilation. *Hydrol. Earth Syst. Sci.* 21, 3687–3700.
572 <https://doi.org/10.5194/hess-21-3687-2017>
573 Akaike, H., 1974. A new look at the statistical model identification. *IEEE transactions on*
574 *automatic control* 19, 716–723.

575 Akaike, H., 1973. Information Theory and an Extension of the Maximum Likelihood Principle",
576 in B. Petrov and B. Csake (eds), Second International Symposium on Information
577 Theory, Akademiai Kiado, Budapest, 267–281.

578 Allamano, P., Laio, F., Claps, P., 2011. Effects of disregarding seasonality on the distribution of
579 hydrological extremes. *Hydrology and Earth System Sciences* 15, 3207–3215.

580 Baratti, E., Montanari, A., Castellarin, A., Salinas, J.L., Viglione, A., Bezzi, A., 2012. Estimating
581 the flood frequency distribution at seasonal and annual time scales. *Hydrology and Earth
582 System Sciences* 16, 4651–4660.

583 Bowers, M.C., Tung, W.W., Gao, J.B., 2012. On the distributions of seasonal river flows:
584 lognormal or power law? *Water Resources Research* 48.

585 Box, G.E.P., Jenkins, G.M., 1970. *Time series analysis: forecasting and control*, 1976. ISBN: 0-
586 8162-1104-3.

587 Buishand, T.A., Demaré, G.R., 1990. Estimation of the annual maximum distribution from
588 samples of maxima in separate seasons. *Stochastic Hydrology and Hydraulics* 4, 89–103.

589 Burnham, K.P., Anderson, D.R., 2004. Multimodel inference understanding AIC and BIC in
590 model selection. *Sociological methods & research* 33, 261–304.

591 Burnham, K.P., Anderson, D.R., 2002. Information and likelihood theory: a basis for model
592 selection and inference. *Model selection and multimodel inference: a practical
593 information-theoretic approach* 49–97.

594 Burt, T.P., Howden, N.J.K., 2011. A homogenous daily rainfall record for the Radcliffe
595 Observatory, Oxford, from the 1820s. *Water Resour. Res.* 47, W09701.
596 <https://doi.org/10.1029/2010WR010336>

597 Chen, D., Chen, H.W., 2013. Using the Köppen classification to quantify climate variation and
598 change: An example for 1901–2010. *Environmental Development* 6, 69–79.
599 <https://doi.org/10.1016/j.envdev.2013.03.007>

600 Chen, L., Guo, S., Yan, B., Liu, P., Fang, B., 2010a. A new seasonal design flood method based
601 on bivariate joint distribution of flood magnitude and date of occurrence. *Hydrological
602 Sciences Journal* 55, 1264–1280. <https://doi.org/10.1080/02626667.2010.520564>

603 Chen, L., Guo, S., Yan, B., Liu, P., Fang, B., 2010b. A new seasonal design flood method based
604 on bivariate joint distribution of flood magnitude and date of occurrence. *Hydrological
605 Sciences Journal–Journal des Sciences Hydrologiques* 55, 1264–1280.

606 Chen, L., Singh, V.P., Guo, S., Fang, B., Liu, P., 2013. A new method for identification of flood
607 seasons using directional statistics. *Hydrological Sciences Journal* 58, 28–40.

608 Chiew, F.H.S., Zhou, S.L., McMahon, T.A., 2003. Use of seasonal streamflow forecasts in water
609 resources management. *Journal of Hydrology* 270, 135–144.

610 Coles, S., Pericchi, L.R., Sisson, S., 2003. A fully probabilistic approach to extreme rainfall
611 modeling. *Journal of Hydrology* 273, 35–50.

612 Cunderlik, J.M., Burn, D.H., 2002. Analysis of the linkage between rain and flood regime and its
613 application to regional flood frequency estimation. *Journal of Hydrology* 261, 115–131.

614 Cunderlik, J.M., Ouarda, T.B., Bobée, B., 2004a. Determination of flood seasonality from
615 hydrological records/Détermination de la saisonnalité des crues à partir de séries
616 hydrologiques. *Hydrological Sciences Journal* 49.

617 Cunderlik, J.M., Ouarda, T.B., Bobée, B., 2004b. Determination of flood seasonality from
618 hydrological records/Détermination de la saisonnalité des crues à partir de séries
619 hydrologiques. *Hydrological Sciences Journal* 49.

620 Cunderlik, J.M., Ouarda, T.B., Bobée, B., 2004c. On the objective identification of flood
621 seasons. *Water Resources Research* 40.

622 Dhakal, N., Jain, S., Gray, A., Dandy, M., Stancioff, E., 2015. Nonstationarity in seasonality of
623 extreme precipitation: A nonparametric circular statistical approach and its application.
624 *Water Resources Research* 51, 4499–4515.

625 Durrans, S.R., Eiffe, M.A., Thomas Jr, W.O., Goranflo, H.M., 2003. Joint seasonal/annual flood
626 frequency analysis. *Journal of Hydrologic Engineering* 8, 181–189.

627 Efstratiadis, A., Koussis, A.D., Koutsoyiannis, D., Mamassis, N., 2014. Flood design recipes vs.
628 reality: can predictions for ungauged basins be trusted? *Natural Hazards and Earth
629 System Sciences* 14, 1417–1428.

630 Fang, B., Guo, S., Wang, S., Liu, P., Xiao, Y., 2007. Non-identical models for seasonal flood
631 frequency analysis. *Hydrological Sciences Journal* 52, 974–991.
632 <https://doi.org/10.1623/hysj.52.5.974>

633 Fisher, R.A., Tippett, L.H.C., 1928. Limiting forms of the frequency distribution of the largest or
634 smallest member of a sample, in: *Mathematical Proceedings of the Cambridge
635 Philosophical Society*. Cambridge Univ Press, pp. 180–190.

636 Golian, S., Saghafian, B., Maknoon, R., 2010. Derivation of Probabilistic Thresholds of Spatially
637 Distributed Rainfall for Flood Forecasting. *Water Resour Manage* 24, 3547–3559.
638 <https://doi.org/10.1007/s11269-010-9619-7>

639 Hirschboeck, K.K., 1988. Flood hydroclimatology. *Flood geomorphology* 27, 49.

640 Jenkinson, A.F., 1955. The frequency distribution of the annual maximum (or minimum) values
641 of meteorological elements. *Quarterly Journal of the Royal Meteorological Society* 81,
642 158–171.

643 Klein Tank, A.M.G., Wijngaard, J.B., Können, G.P., Böhm, R., Demarée, G., Gocheva, A.,
644 Mileta, M., Pashiardis, S., Hejkrlik, L., Kern-Hansen, C., 2002. Daily dataset of 20th-
645 century surface air temperature and precipitation series for the European Climate
646 Assessment. *International journal of climatology* 22, 1441–1453.

647 Koutsoyiannis, D., 2004a. Statistics of extremes and estimation of extreme rainfall: I. Theoretical
648 investigation/Statistiques de valeurs extrêmes et estimation de précipitations extrêmes: I.
649 Recherche théorique. *Hydrological sciences journal* 49.

650 Koutsoyiannis, D., 2004b. Statistics of extremes and estimation of extreme rainfall: II. Empirical
651 investigation of long rainfall records/Statistiques de valeurs extrêmes et estimation de
652 précipitations extrêmes: II. Recherche empirique sur de longues séries de précipitations.
653 *Hydrological Sciences Journal* 49.

654 Koutsoyiannis, D., Yao, H., Georgakakos, A., 2008. Medium-range flow prediction for the Nile:
655 a comparison of stochastic and deterministic methods/Prévision du débit du Nil à moyen
656 terme: une comparaison de méthodes stochastiques et déterministes. *Hydrological
657 Sciences Journal* 53, 142–164.

658 Kutiel, H., Trigo, R.M., 2014. The rainfall regime in Lisbon in the last 150 years. *Theoretical
659 and applied climatology* 118, 387–403.

660 Laio, F., Di Baldassarre, G., Montanari, A., 2009. Model selection techniques for the frequency
661 analysis of hydrological extremes. *Water Resources Research* 45.

662 Leadbetter, M.R., 1974. On extreme values in stationary sequences. *Probability theory and
663 related fields* 28, 289–303.

- 664 Lee, J.-J., Kwon, H.-H., Kim, T.-W., 2012. Spatio-temporal analysis of extreme precipitation
665 regimes across South Korea and its application to regionalization. *Journal of hydro-*
666 *environment research* 6, 101–110.
- 667 Li, J., Thyer, M., Lambert, M., Kuzera, G., Metcalfe, A., 2016. Incorporating seasonality into
668 event-based joint probability methods for predicting flood frequency: A hybrid causative
669 event approach. *Journal of Hydrology* 533, 40–52.
670 <https://doi.org/10.1016/j.jhydrol.2015.11.038>
- 671 MacQueen, J., 1967. Some methods for classification and analysis of multivariate observations,
672 in: *Proceedings of the Fifth Berkeley Symposium on Mathematical Statistics and*
673 *Probability*. Oakland, CA, USA, pp. 281–297.
- 674 Marani, M., Zanetti, S., 2015. Long-term oscillations in rainfall extremes in a 268 year daily time
675 series. *Water Resources Research* 51, 639–647.
- 676 Mascaro, G., 2018. On the distributions of annual and seasonal daily rainfall extremes in central
677 Arizona and their spatial variability. *Journal of Hydrology* 559, 266–281.
678 <https://doi.org/10.1016/j.jhydrol.2018.02.011>
- 679 Menne, M.J., Durre, I., Vose, R.S., Gleason, B.E., Houston, T.G., 2012. An Overview of the
680 Global Historical Climatology Network-Daily Database. *J. Atmos. Oceanic Technol.* 29,
681 897–910. <https://doi.org/10.1175/JTECH-D-11-00103.1>
- 682 Ntegeka, V., Willems, P., 2008. Trends and multidecadal oscillations in rainfall extremes, based
683 on a more than 100-year time series of 10 min rainfall intensities at Uccle, Belgium.
684 *Water Resources Research* 44.
- 685 Papalexiou, S.M., Koutsoyiannis, D., 2016. A global survey on the seasonal variation of the
686 marginal distribution of daily precipitation. *Advances in Water Resources* 94, 131–145.
- 687 Papalexiou, S.M., Koutsoyiannis, D., 2013. Battle of extreme value distributions: A global
688 survey on extreme daily rainfall. *Water Resources Research* 49, 187–201.
- 689 Parajka, J., Kohnová, S., Bálint, G., Barbuc, M., Borga, M., Claps, P., Cheval, S., Dumitrescu,
690 A., Gaume, E., Hlavčová, K., others, 2010. Seasonal characteristics of flood regimes
691 across the Alpine–Carpathian range. *Journal of hydrology* 394, 78–89.
- 692 Parajka, J., Kohnová, S., Merz, R., Szolgay, J., Hlavčová, K., Blöschl, G., 2009. Comparative
693 analysis of the seasonality of hydrological characteristics in Slovakia and
694 Austria/Analyse comparative de la saisonnalité de caractéristiques hydrologiques en
695 Slovaquie et en Autriche. *Hydrological Sciences Journal* 54, 456–473.
- 696 Pryor, S.C., Schoof, J.T., 2008. Changes in the seasonality of precipitation over the contiguous
697 USA. *J. Geophys. Res.* 113, D21108. <https://doi.org/10.1029/2008JD010251>
- 698 Rust, H.W., Maraun, D., Osborn, T.J., 2009. Modelling seasonality in extreme precipitation. *The*
699 *European Physical Journal-Special Topics* 174, 99–111.
- 700 Serinaldi, F., Kilsby, C.G., 2014. Rainfall extremes: Toward reconciliation after the battle of
701 distributions. *Water resources research* 50, 336–352.
- 702 Sivapalan, M., Blöschl, G., Merz, R., Gutknecht, D., 2005. Linking flood frequency to long-term
703 water balance: Incorporating effects of seasonality. *Water Resources Research* 41.
- 704 Tye, M.R., Blenkinsop, S., Fowler, H.J., Stephenson, D.B., Kilsby, C.G., 2016. Simulating
705 multimodal seasonality in extreme daily precipitation occurrence. *Journal of Hydrology*
706 537, 117–129.
- 707 Villarini, G., 2012. Analyses of annual and seasonal maximum daily rainfall accumulations for
708 Ukraine, Moldova, and Romania. *Int. J. Climatol.* 32, 2213–2226.
709 <https://doi.org/10.1002/joc.3394>

710 Von Mises, R., 1936. La distribution de la plus grande de n valeurs. Rev. math. Union
711 interbalcanique 1.
712 Wang, Q.J., Robertson, D.E., Chiew, F.H.S., 2009. A Bayesian joint probability modeling
713 approach for seasonal forecasting of streamflows at multiple sites. Water Resources
714 Research 45.
715 Wu, H., Qian, H., 2017. Innovative trend analysis of annual and seasonal rainfall and extreme
716 values in Shaanxi, China, since the 1950s. Int. J. Climatol. 37, 2582–2592.
717 <https://doi.org/10.1002/joc.4866>
718

719 **Tables**

720 **Table 1** Characteristics of the 27 daily rainfall stations used in the analysis. The last column
721 shows the final number of years that were accepted for the analysis after quality control.

Stations	Country	Latitude	Longitude	Start year	End year	Years accepted
Bologna	Italy	44.5	11.346	1813	2007	195
Palermo	Italy	38.11	13.351	1797	2008	175
Mantova	Italy	45.158	10.797	1840	2008	160
Milan	Italy	45.472	9.1892	1858	2008	151
Genoa	Italy	44.414	8.9264	1833	2008	176
Florence	Italy	43.8	11.2	1822	1979	155
Padua	Italy	45.866	11.526	1725	2013	275
Newcastle	Australia	-32.919	151.8	1862	2015	151
Deniliquin	Australia	-35.527	144.95	1858	2014	154
Melbourne	Australia	-37.807	144.97	1855	2015	160
Robe	Australia	-37.163	139.76	1860	2015	152
Sydney	Australia	-33.861	151.21	1858	2015	157
Jena Sternwarte	Germany	50.927	11.584	1826	2015	179
Hohenpeissenberg	Germany	47.802	11.012	1781	2015	182
Armagh	UK	54.35	-6.65	1838	2001	164
Radcliffe	UK	51.761	-1.2639	1827	2014	188
Zagreb	Croatia	45.817	15.978	1860	2015	154
Vlissingen	Netherlands	51.441	3.5956	1854	2015	158
Eelde	Netherlands	53.124	6.5847	1846	2015	169
Den Helder	Netherlands	52.933	4.75	1850	2015	165
Helsinki	Finland	60.167	24.933	1845	2015	171
Lisbon	Portugal	39.2	-9.25	1863	2013	150
Prague	Czech republic	50.051	14.246	1804	2014	211
Uppsala	Sweden	59.86	17.63	1836	2014	179
Stykkisholmur	Iceland	65.083	-22.733	1856	2015	160
Athens	Greece	37.973	23.72	1863	2014	152

Toronto	Canada	43.667	-79.4	1840	2015	162
---------	--------	--------	-------	------	------	-----

722

723 **Table 2** Δ AIC differences among the seasonal models (one, two or three seasons) under Average
724 Based (AB) and Complete Data (CD) methods. A zero Δ AIC value indicates the model with the
725 smallest AIC value which stands for the best model.

Stations	AB method			CD method					
	Uniform distribution			Weibull distribution			Gamma distribution		
	<i>Number of seasons</i>			<i>Number of seasons</i>					
	1	2	3	1	2	3	1	2	3
Bologna	0	0.047	2.9	27.55	27.51	35.12	0	4.91	9.04
Palermo	5.29	0	1.72	0	50.32	41.37	0.372	9.6	5.15
Mantova	0	0.414	3.92	28.22	25.76	13.43	0	8.58	7.12
Milan	0	0.639	3.86	8.633	10.75	0	30.72	33.5	34.7
Genoa	3.38	0	0.67	9.215	0	6.641	5.797	10.5	18
Florence	1.85	0	3.62	15.52	8.421	0	48.55	54.8	9.9
Padua	0	1.058	4.914	0	9.72	11.12	100.19	56.43	65.84
Newcastle	0.75	0	3.88	60.23	34.25	40.68	8.414	0	15.7
Deniliquin	0	2.894	6.41	18.11	16.3	20.18	0	3.68	9.11
Melbourne	0	0.903	4.58	139.1	76.04	78.35	37.31	0	5.27
Robe	1.45	0	5.09	3.475	36.71	40.45	0	1.7	7.29
Sydney	0	0.556	2.88	37.92	40.93	41.35	0	0.02	2.24
Jena Sternwarte	4.6	0	3.69	208.1	123.2	131.6	46.77	0	1.45
Hohenpeissenberg	5.5	0	3.25	85.83	63.77	67.7	0	8.93	6.95
Armagh	0	0.78	3.71	161.3	103.2	106.9	3.412	0	3.04
Radcliffe	0	0.682	3.68	129.6	70.5	77.79	0	0.74	0.75
Zagreb	0.5	0	3.68	42.95	17.99	23.94	0	19.9	25.87
Vlissingen	0.66	0	3.34	78.03	36.79	36.18	0	4.02	9.84
Eelde	1.79	0	3.55	135.8	61.08	67.77	3.338	0	6.24
Den Helder	0.36	0	3.7	201.4	137.5	118.7	27.93	3.58	0
Helsinki	1.9	0	3.69	108.9	48.3	35.58	1.161	0	6.95
Lisbon	8.18	0	7.07	58.26	0	3.646	72.71	7.33	3.04
Prague	2.7	0	1.44	133.3	64.84	58.67	36.75	0.06	0
Uppsala	4.73	0	3.17	187	72.35	58.84	27.02	0.38	0
Stykkisholmur	0	0.657	4.39	103.1	75.99	82.57	2.13	0	6.42
Athens	8.11	0	2.81	104	19.73	23.16	65.54	0	1.45
Toronto	0	1.704	5.14	183.5	121.3	113.1	18.24	0	2.2

726 **Table 3** Temporal changes in seasonality identified by application of Average Based (AB) and
 727 Complete Data (CD) methods for non-overlapping sub-periods for the four longest stations of the
 728 dataset. For the longer station of Padua, an additional sub-period is investigated (4th window).

Station	Record length	Number of Seasons							
		1 st window		2 nd window		3 rd window		4 th window	
		Method		Method		Method		Method	
		AB	CD	AB	CD	AB	CD	AB	CD
Padua	1725-2013	1	1	1	1	1	1	1	1
Bologna	1813-2007	1	1	2	1	1	1	–	–
Radcliffe	1827-2014	1	1	1	1	1	1	–	–
Prague	1804-2014	2	1	2*	2*	2	2	–	–
<i>Span of wet season in months for Prague</i>									
		5-8	–	5-9	5-9	5-8	5-8	–	–

729

730 **Table 4** Comparative statistics of the GEV annual and seasonal parameters, i.e., shape parameter
 731 κ , scale parameter σ and location parameter ψ , as estimated via Maximum Likelihood method for
 732 the stations in which two or three seasons are identified by Average Based (AB) and Complete
 733 Data (CD) methods. The last column of each table shows the percentage (%) of stations in which
 734 the parameter value for the wet season is higher than the corresponding value for the dry season.

AB method (16 stations)					CD method (16 stations)			
Parameter	Annual	Wet season	Dry season	Parameter Variation: (wet>dry)%	Annual	Wet season	Dry season	Parameter Variation: (wet>dry)%
Mean	0.1121	0.091	0.097	62.5	0.115	0.106	0.104	45
κ Percent Positive	93.8	93.8	87.5	-	93.8	93.8	75	-
σ Mean	12.207	12.706	8.747	93.8	12.187	13.238	9.2872	100
ψ Mean	39.265	35.602	23.772	100	39.652	40.998	34.333	100

735

736 **Table 5** Statistics of the GEV parameters, i.e., shape parameter κ , scale parameter σ and location
 737 parameter ψ , as estimated for the Annual Maxima series for all stations (27) via Maximum
 738 Likelihood (ML), method of moments (MM) and Least Squares method (LS).

Parameter of the annual model		ML	MM	LS
κ	Mean	0.099	0.062	0.120
	Percent Positive	92.6	88.9	96.3
σ	Mean	12.638	10.500	12.732
ψ	Mean	40.510	42.246	40.295

739

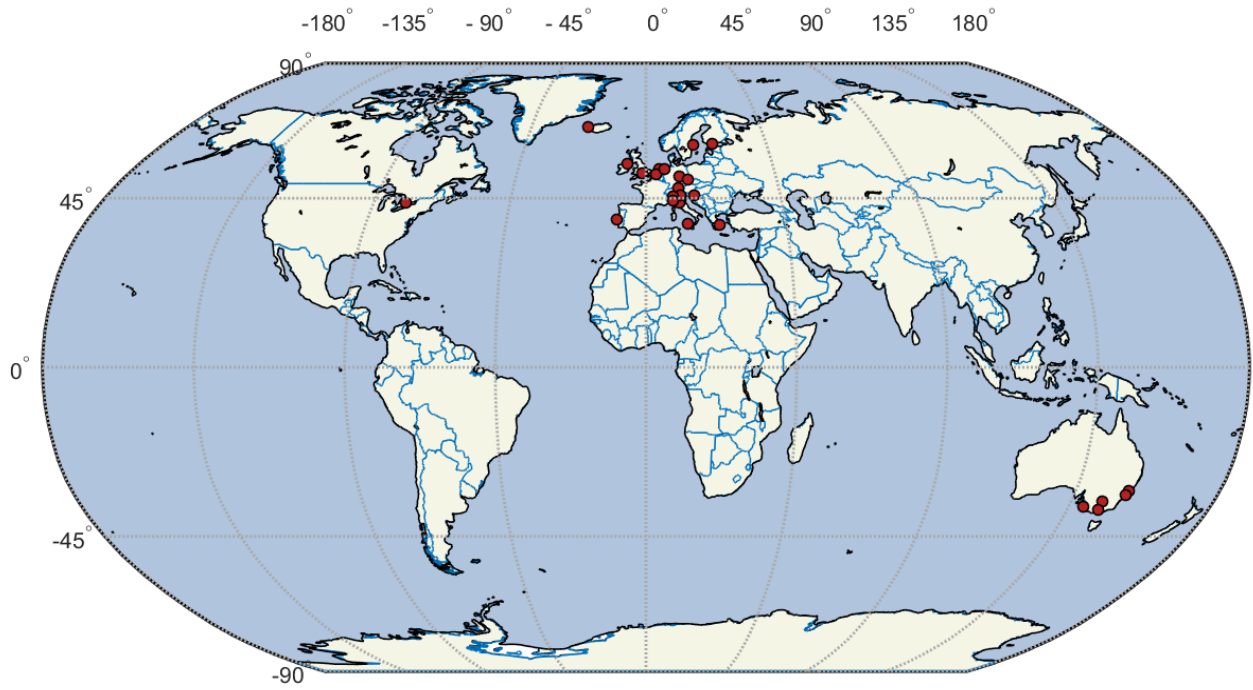
740

741

742

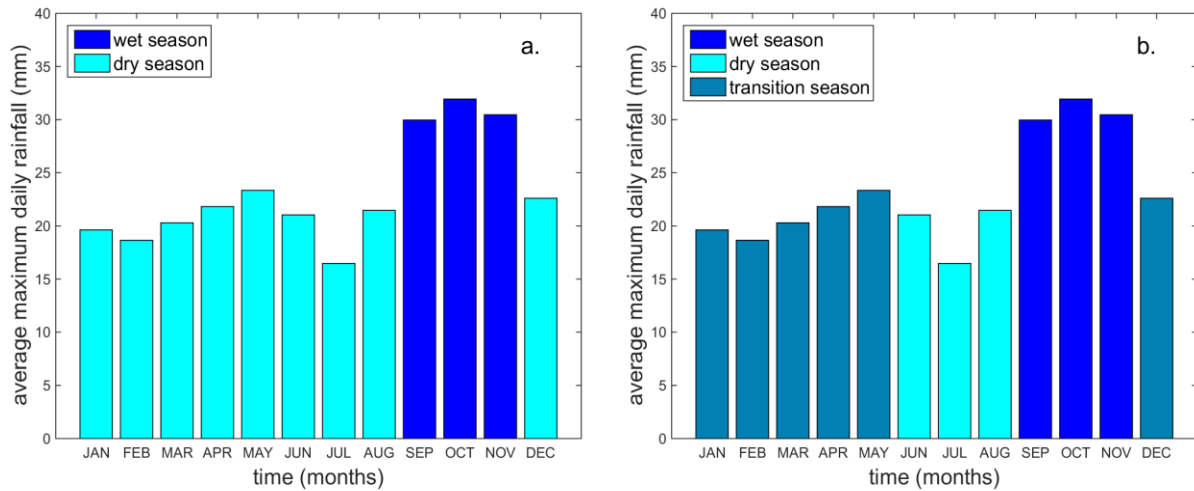
743

744 **Figures**

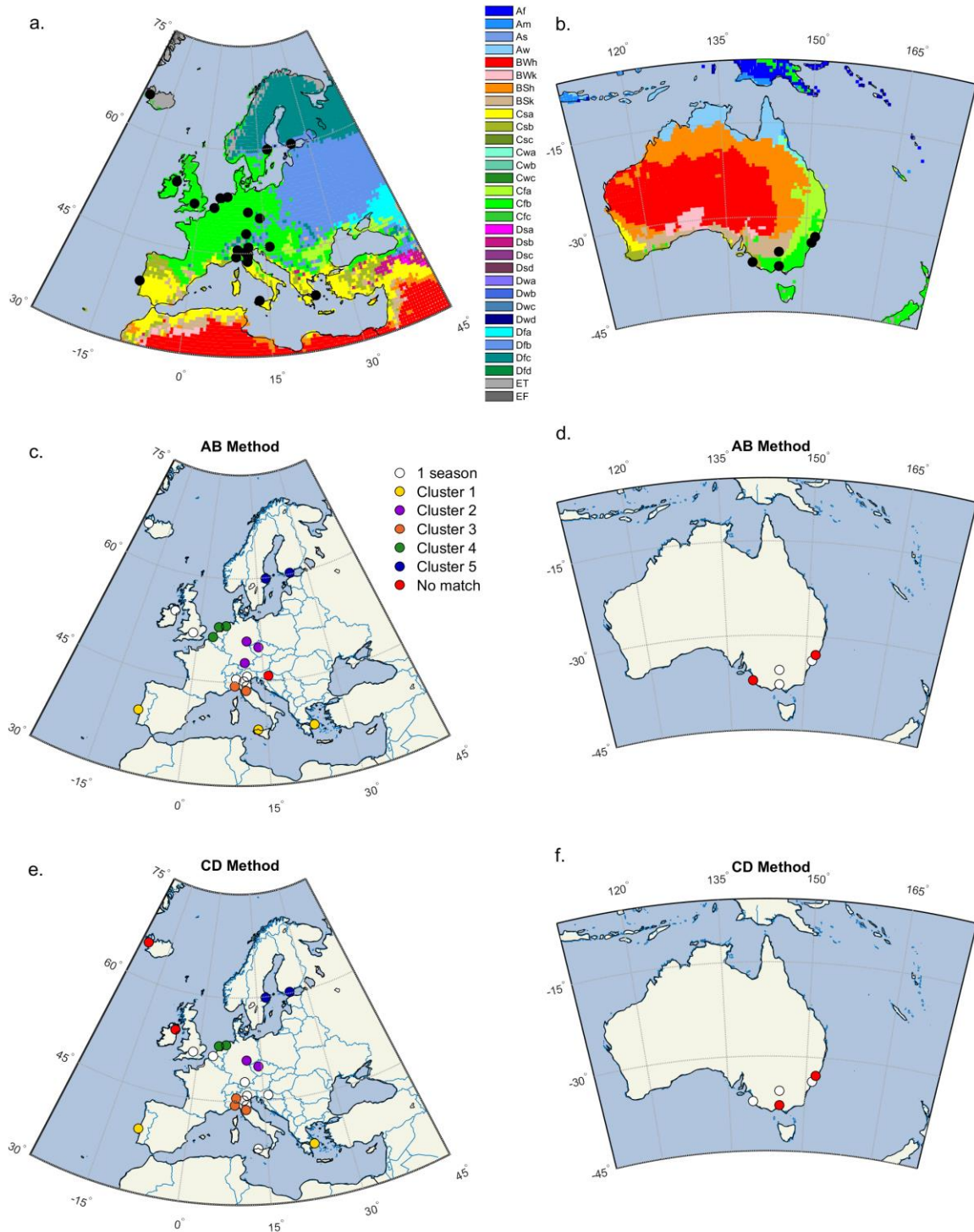


745 **Figure 1.** Map of the 27 analyzed stations with daily rainfall records spanning over 150 years.
746

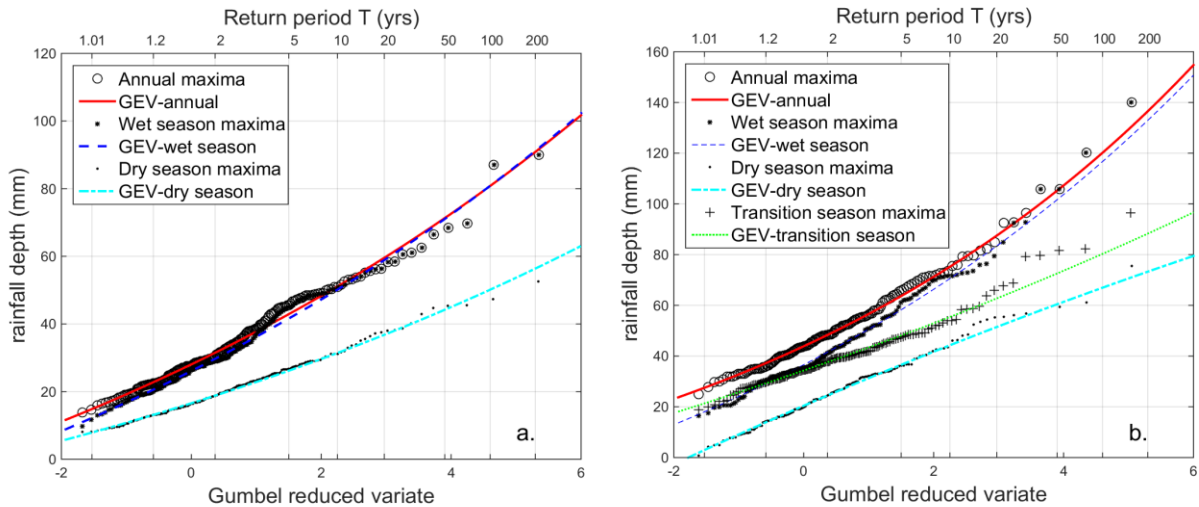
747



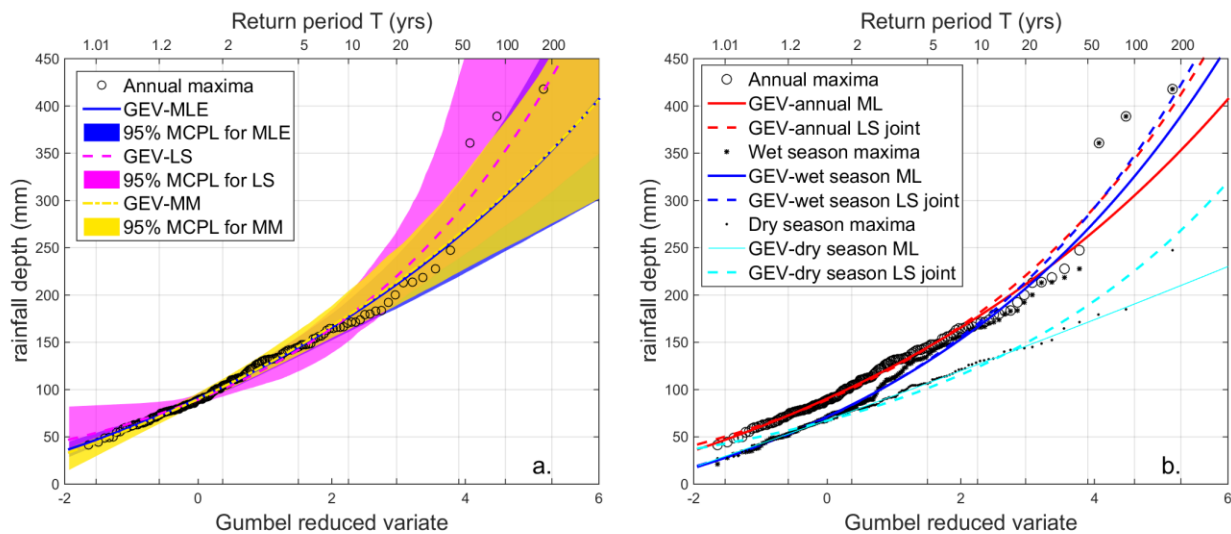
748 **Figure 2.** Climatograms showing the partition in two seasons (a) and three seasons (b) after
749 application of the SSD clustering algorithm for the station of Florence.
750



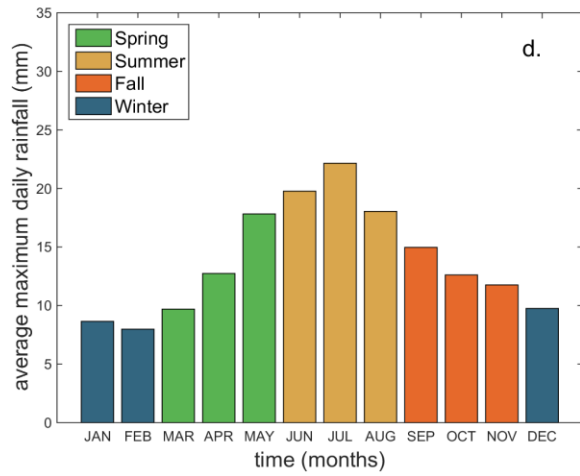
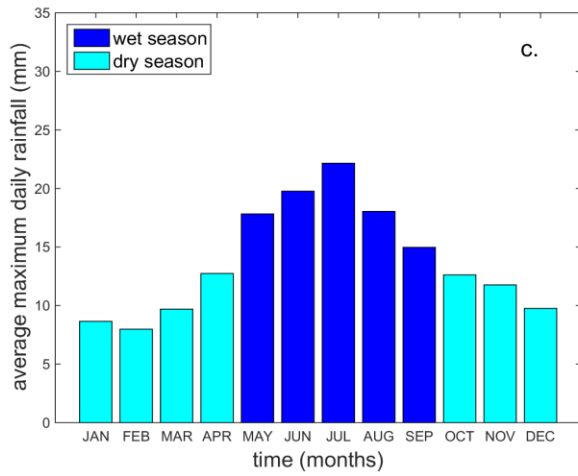
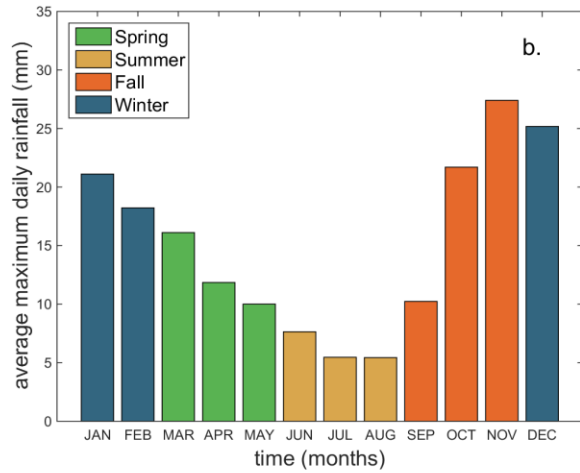
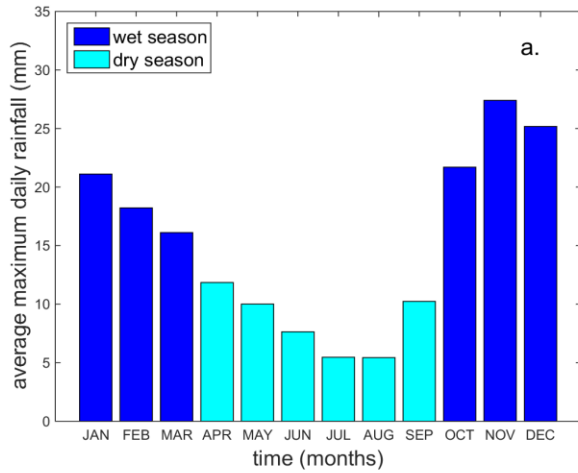
751
 752 **Figure 3.** Spatial and climatological coherence of the identified seasons for the regions of
 753 Europe (a,c,e) and Australia (b,d,f). Figures a,b show the location of the stations on a Köppen
 754 climatological map, while the rest show the stations clustered by similarity. White dots represent
 755 stations having one season; the remaining dots denote stations having at least 60% overlap of
 756 months belonging to the wet season. Red dots denote stations with a lower percentage of
 757 similarity to their neighboring stations.



758
 759 **Figure 4.** Gumbel probability plots of the fitting of the GEV distribution to the annual maxima
 760 (red solid line), to the wet season maxima (blue dashed line) and to the dry season maxima (cyan
 761 dash-dotted line) for the stations of Prague (a) and Florence (b). For the station of Florence (b),
 762 the fitting of the GEV distribution to the transition season maxima (green dotted line) is also
 763 shown.

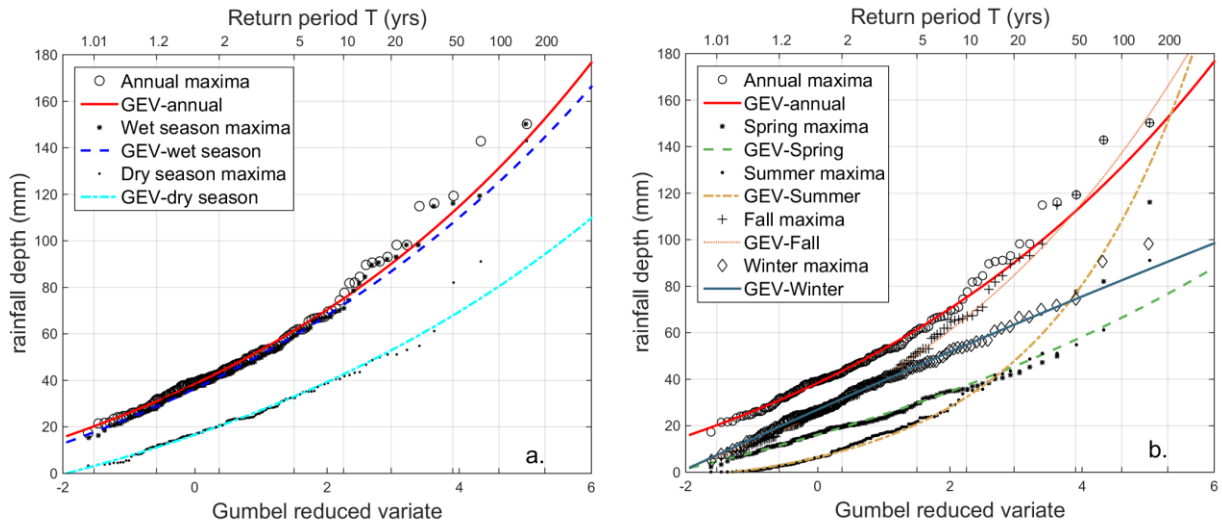


764
 765 **Figure 5.** Gumbel probability plot of the fitting of the GEV distribution to the annual maxima by
 766 the maximum likelihood method (blue color), least-squares method (magenta color) and method
 767 of moments (yellow color) along with 95% Monte Carlo Prediction Limits (MCPL) for each
 768 method for the station of Genoa (a). The crossing over distance observed in the area of high
 769 return periods, where the wet-season probability line (blue solid line) crosses the annual
 770 probability line (red solid line), is greatly eliminated when a common shape parameter is
 771 employed via the least-squares method (b).



772
 773 **Figure 6.** Partition in seasons resulting from application of the proposed season identification
 774 method versus the fixed 4-season partition for the stations of Athens (a, b respectively) and Jena
 775 (c, d respectively).

776



777

778 **Figure 7.** Gumbel probability plots of the fitting of the GEV distribution to the annual and
 779 seasonal maxima resulting from the proposed season identification method (a) vs Gumbel
 780 probability plot of the fitting of the GEV distribution to the annual and seasonal maxima
 781 according to the fixed 4-season partition (b) for the station of Athens.

782